Facultad de Biología

Departamento de Microbiología

La Familia de proteínas Hha-YmoA: estudios estructurales y papel regulador en *Yersinia enterocolitica*

Programa de Doctorado: Microbiología Ambiental y Biotecnología (2001-2003).

Conformidad del director de tesis

Memoria presentada por J. Ignacio Pons Ximénez para optar al título de Doctor por la Universidad de Barcelona

Dr. Antonio Juárez Giménez

J. Ignacio Pons Ximénez

Barcelona, 2006

7.- ANEXO

Available online at www.sciencedirect.com
SCIENCE DIRECT®
Protein Expression and Purification 35 (2004) 293–297
Protein Expression & Purification
www.elsevier.com/locate/yprep

In vivo increase of solubility of overexpressed Hha protein by tandem expression with interacting protein H-NS

José I. Pons, Sonia Rodríguez, Cristina Madrid, Antonio Juárez, and José M. Nieto*

Department of Microbiology, Faculty of Biology, University of Barcelona, Avda. Diagonal, 645, 08028 Barcelona, Spain

Received 12 November 2003, and in revised form 25 February 2004

Abstract

Gene cloning in appropriate vectors followed by protein overexpression in *Escherichia coli* is the common means for protein purification. This approach has many advantages but also some drawbacks; one of these is that many proteins fail to achieve a soluble conformation when overexpressed in *E. coli*. Hha protein belongs to a family of nucleoid-associated proteins functionally related to the H-NS family of proteins. Hha-like proteins and H-NS-like proteins are able to semidirectly bind to each other. We show in this work that overexpressed Hha or HisHha protein (a functional derivative of Hha containing a 6× His tag at the amino end) from a T7-polymerase promoter in BL21 DE3 *E. coli* strains results in the vast majority of the protein accumulated in insoluble aggregates (inclusion bodies). We also show that tandem overexpression of HisHha and H-NS increases the solubility of HisHha and prevents the formation of inclusion bodies. Single amino acid substitutions in the HisHha protein, which impair interaction with H-NS, render insoluble protein even when tandem-expressed with H-NS, tandem expression of an insoluble protein and an interacting partner is an experimental strategy which could be useful to increase the solubility of other overexpressed proteins in *E. coli*.

Keywords: Protein solubility; Hha; H-NS

The study of the structure of a protein often requires as a first step the production of large amounts of the protein of interest in *Escherichia coli*. However, frequently the overexpression of a protein in *E. coli* results in the production of insoluble aggregates of non-functional protein (inclusion bodies) due to the loss of solubility of misfolded polypeptides. Such inclusion bodies can sometimes represent an easy way to purify a protein, but this approach has a serious drawback: it has to be followed by the appropriate solubilization procedure with strong chaotropic denaturants and refolding by dilution or dialysis with optimized refolding buffers. Many polypeptides particularly those containing disulfide bonds will not easily recover their native conformation after such an approach. Thus, whenever possible, obtaining a high level of production of soluble (i.e., correctly folded) protein in *E. coli* in the first place is the best approach to protein purification for structural studies. Increase of expression of high amounts of soluble proteins in *E. coli* has been obtained through different strategies which include alteration of growth conditions, co-expression of chaperones, and the use of fusion proteins [1–3].

The Hha protein is a small polypeptide of 8.5 kDa involved in the regulation of gene expression of different virulence factors in *E. coli* [4] and *Yersinia enterocolitica* [5]. The H-NS family of proteins conform to a well-known histone-like class of structural proteins broadly represented in the Gram-negative bacteria [6]. We have reported that the Hha protein interacts with the H-NS protein to regulate expression of virulence factor α-hemolysin of *E. coli* [7,8].

The physical and chemical context which a protein encounters when overexpressed in *E. coli* is critical for solubility to be attained. This includes the interactions with chaperon proteins or other proteins. In this paper, we report our finding that overexpression of Hha results in the formation of insoluble aggregates but tandem expression of Hha and H-NS greatly increases the

* Corresponding author. Fax: +34934034629.
E-mail address: jmnieto@ub.edu (J.M. Nieto).

1046-5928/$ - see front matter © 2004 Elsevier Inc. All rights reserved.
doi:10.1016/j.pep.2004.02.018

solubility of Hha. We provide data to support that the interaction between both proteins is an essential factor to achieve such effect.

Materials and methods

Escherichia coli bacterial strains were cultured and manipulated according to standard microbiological procedures. *E. coli* strain BL21 DE3 pLysE was the host of the T7 polymerase promoter system expression experiments [9].

Plasmid pETHISHHA contains the *hishha* recombinant gene encoding a completely functional HisHha protein composed of the native Hha protein of *E. coli* preceded by a Met and six His amino acids, under the control of the T7 polymerase promoter of pET3b [7]. The *hns* gene of *E. coli* was PCR amplified with oligonucleotides HNSBPROX (5′-GAATTTAAGGATCCAT TATTACC-3′) and HNSBDIST (5′-CCGGACAATAA AGGATCCCGC-3′) and cloned in the *Bam*HI target positioned at the end of the *hha* gene in plasmid pETHISHHA. The resulting plasmid was named pETHISHHAHNS. In this plasmid, the initial Met codon of the *hns* gene (sequence accession X57231) is positioned 73 bp after the final Arg codon of the *hha* gene, and both genes are positioned under the control of the T7 promoter as a bicistronic unit (Fig. 1). A DNA cassette including the *lac*O operator sequence was obtained by annealing oligonucleotides LACOF (5′-CTAGAATTG TGAGCGGATAACAATT-3′) and LACOR (5′-TAGA ATTGTTATCCGCTCACAATT-3′) and then inserted at the *Xba*I site after the T7 polymerase promoter sequence of plasmid pETHISHHA derivatives, thus permitting a lower level of background expression before IPTG-induction (Fig. 1)

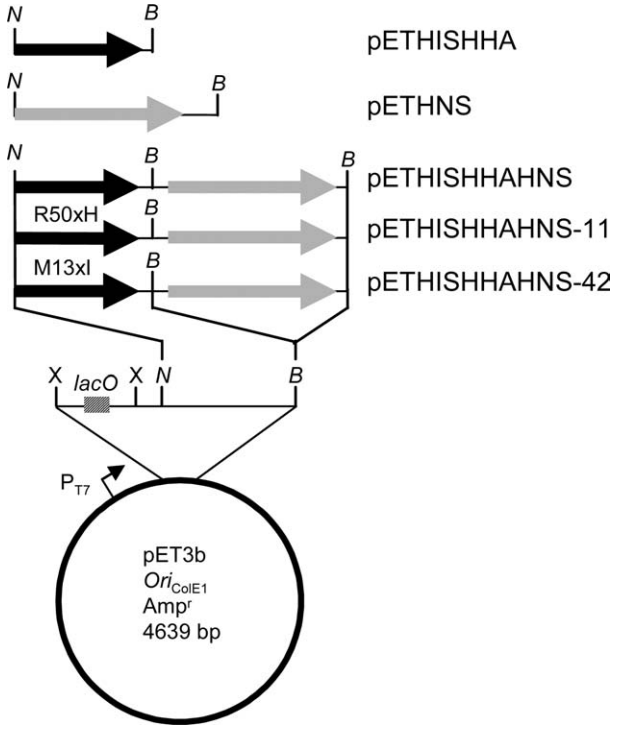

Fig. 1. Schematic diagram of the single and tandem expression constructs. N, *Nde*I; X, *Xba*I; B, *Bam*HI. Black line, *hishha* gene; grey line, *hns* gene.

Plasmid pETHISHHA-11 is equivalent to pETHISHHA except that the *hha*-11 gene contains a single base substitution (CGC to CAC) which results in an amino acid change in the encoded protein (R50 to H) rendering it unable to bind H-NS [8]. Plasmid pETHISHHA-42 is also equivalent to pETHISHHA except that in this case the *hha*-42 gene contains a single base substitution (ATG to ATA) which results in an amino acid change in the encoded protein (M13 to I) but renders a protein capable of binding H-NS (our unpublished results). Plasmids pETHISHHAHNS-11 and pETHISHHAHNS-42 (Fig. 1) were constructed by adding at the *Bam*HI site of pETHISHHA-11 and pETHISHHA-42 a DNA fragment containing the *hns* gene of *E. coli* obtained by PCR amplification with oligonucleotides HNSBPROX and HNSBDIST and digestion with *Bam*HI. Plasmid pETHNS contains the *hns* gene cloned between the *Nde*I (overlapping the initial Met codon of *hns*) and *Bam*HI sites of pET3b. It was obtained after PCR amplification of the *hns* gene of *E. coli* with oligonucleotides HNSNPROX (5′-GAGAT TACTCATATGAGCG-3′) and HNSBDIST, followed by digestion of the PCR product with *Nde*I and *Bam*HI and cloning in equally digested pET3b plasmid.

According to conventional procedures, exponential cultures of the *E. coli* BL21 DE3 pLysE strain were made competent by washing with cold calcium chloride (200 mM) and transformed with the appropriate expression plasmid. Fresh transforming colonies were obtained for every experiment. Colonies were inoculated in fresh LB medium (10 g/L tryptone, 10 g/L yeast extract, and 5 g/L NaCl) plus ampicillin (50 μg/ml) to an initial OD_{600} of 0.1. Growth was at 37 °C, in conic flasks with aeration (200 rpm) until OD_{600} reached 1.0 and then IPTG was added to a final concentration of 0.5 mM. Cultures were further incubated in the same conditions for 3 h. Cultures obtained this way were used either for electron microscopy studies or for SDS–PAGE analysis.

Electron microscopy of BL21 DE3 pLysE cells containing either plasmid pETHISHHA or pETHISHHAHNS was performed as follows. Cultures were obtained and protein synthesis was induced with IPTG for 3 h. Cells pellets were obtained by centrifugation and bacteria were fixed overnight in 2% glutaraldehyde, 0.1 M phosphate buffer, pH 7.4, and then treated for 4 h with 1% osmium tetroxide, 0.8% potassium ferricyanide, and 0.1 M phosphate buffer, pH 7.4. Afterwards, the cells were dehydrated by washing with a graded series of acetone and then embedded in Spurr resin at room

temperature for three days. Ultrathin sections were placed on copper grids and treated with uranyl acetate and lead citrate. Examination was done with a Jeol 1010 electron microscope.

Continuous production of the proteins was monitored by SDS–PAGE analysis of whole cells from samples obtained at 30 min time intervals. After 3 h of induction, aliquots of 1 ml of the culture were centrifuged and cells were resuspended in an equal volume of 20 mM Hepes, pH 7.9. Cells were disrupted by sonication and then the soluble and insoluble fractions were separated by centrifugation at 15,000*g*. Comparable amounts of each fraction were boiled in denaturing sample buffer and analyzed by denaturing SDS–PAGE [10]. Proteins were stained with Coomassie brilliant blue. Immunoblotting with anti-Hha and anti-H-NS antiserum [8] was performed according to standard methodology.

Results and discussion

Although a small proportion of the protein remains soluble and can be then purified by nickel–nitrilotriacetic acid metal-affinity chromatography [7], overexpression of the HisHha recombinant protein from the strong T7 promoter of plasmid pETHISHHA results in the accumulation of most of the protein in insoluble aggregates: transmission electron micrographs of *E. coli* BL21 DE3 pLysE pETHISHHA grown for 3 h at 37 °C under 0.5 mM IPTG induction conditions reveal the formation of inclusion bodies (Fig. 2A), and SDS–PAGE analysis of the fractions of the cells obtained after sonication and centrifugation further indicates that most of the HisHha protein aggregates under these conditions (Figs. 3A and F).

Previous results obtained in our laboratory suggested that the solubility of overexpressed HisHha protein might be affected by the balance between rate of monomer synthesis and hetero-oligomerization as a result of its interaction with H-NS. To test this possibility, we have constructed different plasmids and used them to overexpress HisHha alone or accompanied by H-NS. Cultures of *E. coli* BL21 DE3 plysE host cells holding plasmid pETHISHHAHNS, which contains the open reading frame encoding the H-NS protein of *E. coli* immediately after the HisHha sequence, were IPTG-induced for 3 h and then examined for inclusion body formation and the soluble and insoluble fractions of the cells were examined by SDS–PAGE. We observed that the cells did not form inclusion bodies (Fig. 2B). Accordingly, a significant increase in the solubility of HisHha was observed in the SDS–PAGE gels, reaching almost half the amount of total HisHha protein produced (Figs. 3B and G). It is worth mentioning at this point that overexpression of H-NS alone from BL21 DE3 pLysE host cells holding pETHNS plasmid in equivalent experimental conditions renders half of the total H-NS protein in the soluble fraction (Figs. 3E and J).

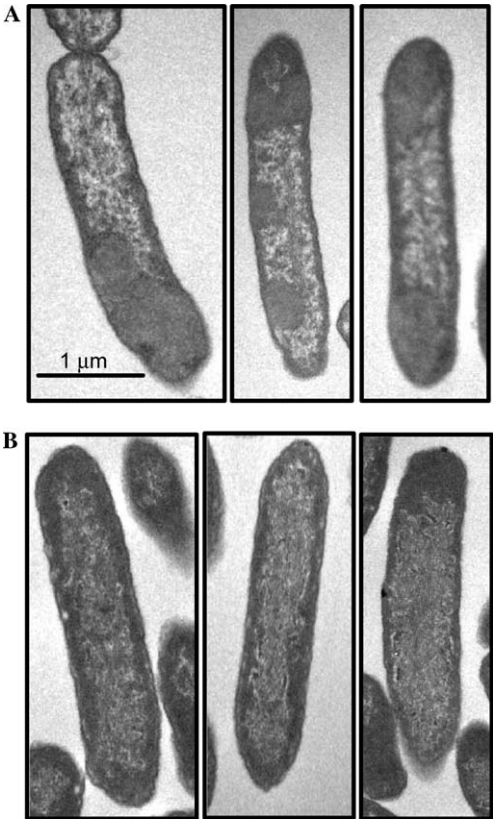

Fig. 2. Transmission electron micrographs of *E. coli* cells holding expression plasmids grown under inducing conditions for 3 h at 37 °C. In both cases (A and B), three representative cells are shown. Magnification is equal for all cells. (A) BL21 DE3 pLysE pETHISHHA cells showing inclusion bodies in the cytoplasm positioned frequently towards the ends of the cell. (B) BL21 DE3 pLysE pETHISHHAHNS cells showing no inclusion bodies.

The results presented above clearly show that co-expression of HisHha and H-NS greatly increases the solubility of the first. However this observation alone does not prove that the interaction between the two proteins and not any other effect due to overexpression of H-NS is the cause of the increased solubility of HisHha. Additional experimental data were gathered from two additional plasmid constructs: pETHISHHAHNS-11 and pETHISHHAHNS-42. Plasmid pETHISHHAHN S-11 is identical in every aspect to pETHISHHAHNS except that the *hha*-11 gene encodes a protein unable to bind H-NS. On the other hand, the *hha*-42 gene in plasmid pETHISHHAHNS-42 encodes a protein with an amino acid substitution too, but in this case does not prevent interaction with H-NS. Cultures of BL21 DE3 pLysE cells holding, respectively, plasmids pETHISHH AHNS-11 and pETHISHHAHNS-42 were IPTG-induced as described and the soluble and insoluble cellular fractions were obtained. SDS–PAGE analysis showed that a minor part of the expressed HisHha-11 remained in the soluble fraction (Figs. 3C and H)

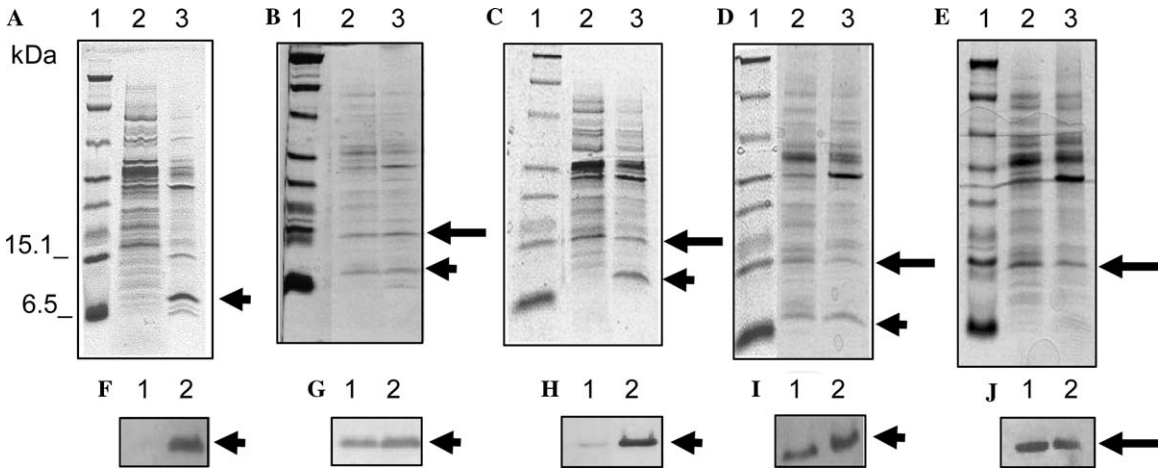

Fig. 3. Coomassie blue-stained SDS–PAGE gels (A–E) and immunoblottings with Hha-specific (F–I) or H-NS-specific antibodies (J) of soluble and insoluble fractions obtained from IPTG-induced overexpression of proteins in BL21 DE3 pLysE *E. coli* cultures containing host cells holding different T7 polymerase expression plasmids: (A) pETHISHHA; (B) pETHISHHAHNS; (C) pETHISHHAHNS-11; (D) pETHISHHAHNS-42; and (E) pETHNS. In (A)–(E), 1, prestained broad range molecular weight marker from Bio-Rad; 2, soluble fraction; and 3, unsoluble fraction. In F–J, 1, soluble fraction; 2, insoluble fraction. Short arrow, HisHha protein; long arrow, H-NS protein.

whereas a major part of the expressed HisHha-42 protein was in the soluble fraction (Figs. 3D and I). This supports that interaction between Hha and H-NS proteins is a *sine qua non* factor for the HisHha proteins to acquire the soluble conformation when overexpressed in tandem with H-NS.

One of the causes of inclusion body formation is protein self-aggregation due to unnatural protein–protein interactions which may appear as a result of the absence of the proper polypeptide folding. Thus, the protein–protein interactions established between the protein being overproduced with itself or with other proteins are of capital importance in the attainability of solubility. An important point to consider is whether this interaction must take place at the same time as the synthesis occurs (in the folding stage) or can occur at a post-synthesis stage. This latter possibility is supported by our finding shown here that H-NS ameliorates the problem of insolubility of overexpressed Hha, yet a complete Hha protein has to be synthesized before interaction can take place, as indicated by the fact that truncations and single amino acid substitutions at the carboxy end (i.e., last synthesized) of the HisHha protein impair the interaction with H-NS [8]. Thus, the effect of H-NS on the solubility of the overproduced HisHha protein is probably exerted at a post-synthesis stage. We propose a model (Fig. 4) to illustrate how these observations could be occurring in the cell. Inclusion bodies in the cell have been found to be dynamic structures and the aggregation of proteins to be reversible in vivo [11], thus, protein aggregation of misfolded HisHha protein could be seen not as a dead-end process but as a transient situation in a cell's cytoplasm where inclusion bodies are continuously being constructed and deconstructed (Fig. 4a and b).

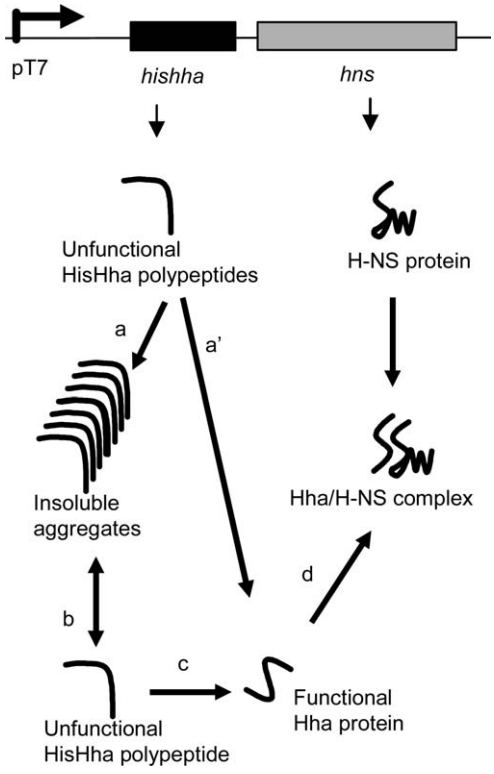

Fig. 4. Schematic model illustrating possible pathways of HisHHA synthesis and solubilization by tandem expression with H-NS in the cytoplasm of BL21 DE3 pLysE host cells holding pETHisHHAHNS plasmid. Most of HisHHA fails to achieve its natural final folding stage, tending to the accumulation of misfolded intermediates (a), although a small portion of the protein can directly reach the soluble conformation (a′). The overexpressed H-NS protein can bind to the soluble HisHha protein (d) thus displacing the equilibrium between the inclusion body and the misfolded monomer (b) by acting as a sink for the correctly folded monomer (c).

The single misfolded polypeptides could in turn be in equilibrium with properly folded HisHha protein (Fig. 4c). In this scenario, the large amount of H-NS in the cells expressing the proteins in tandem would act as a sink for the correctly folded protein (Fig. 4d) and thus displace the equilibrium between the non-functional and functional HisHha proteins (Fig. 4c) and, as a consequence, the equilibrium between the insoluble aggregates and the non-functional HisHha polypeptide (Fig. 4b).

Whether there is a real intermediate aggregation stage of HisHha (Fig. 4a) previous to solubilization by co-expressed H-NS or, on the other hand, the H-NS protein causes the newly formed HisHha protein to adopt the right fold (Fig. 4a′) is difficult to predict from the data shown here and would need further experimental evidence.

The results presented in this paper show an experimental approach for reversion of protein aggregation processes. This could find an application as a therapeutic approach to protein aggregation diseases. From the biotechnological point of view, the increase of solubility by tandem expression of interacting proteins represents another tool in the armamentarium to achieve the production of soluble proteins in *E. coli*, in agreement with published observations of other authors [12–14].

Acknowledgments

This work was supported by Grant No. BIO2001-3499 from the Ministry of Science and Technology of Spain. José I. Pons was the recipient of a Research and Teaching Grant from the University of Barcelona. Sonia Rodríguez was the recipient of a FI grant from the Generalitat of Catalonia. We thank Carmen López and Elisenda Coll for their help in preparation of the samples for the electron microscopy experiments.

References

[1] P. Goloubinoff, A.A. Gatenby, G.H. Lorimer, GroE heat shock proteins promote assembly of foreign prokaryotic ribulose bisphosphate carboxylase oligomers in *Escherichia coli*, Nature 337 (1989) 44–47.

[2] C.W. Goulding, L.J. Perry, Protein production in *Escherichia coli* for structural studies by X-ray crystallography, J. Struct. Biol. 142 (2003) 133–143.

[3] K. Nishihara, M. Kanemori, H. Yanagi, T. Yura, Overexpression of trigger factor prevents aggregation of recombinant proteins in *Escherichia coli*, Appl. Environ. Microbiol. 66 (2000) 884–889.

[4] J.M. Nieto, M. Carmona, S. Bolland, Y. Jubete, F. de La Cruz, A. Juárez, The *hha* gene modulates haemolysin expression in *Escherichia coli*, Mol. Microbiol. 5 (1991) 1285–1293.

[5] A.V. Mikulkis, G.R. Cornelis, A new class of proteins regulating gene expression in enterobacteria, Mol. Microbiol. 11 (1994) 77–86.

[6] C. Tendeng, P. Bertin, H-NS in Gram-negative bacteria: a family of multifaceted proteins, Trends Microbiol. 11 (2003) 511–518.

[7] J.M. Nieto, C. Madrid, A. Prenafeta, E. Miquelay, C. Balsalobre, M. Carrascal, A. Juárez, Expression of the hemolysin operon in *Escherichia coli* is modulated by a nucleoid-protein complex that includes the proteins Hha and H-NS, Mol. Gen. Genet. 263 (2000) 349–358.

[8] J.M. Nieto, C. Madrid, E. Miquelay, J.L. Parra, S. Rodríguez, A. Juárez, Evidence for direct protein–protein interaction between members of the enterobacterial Hha/YmoA and H-NS families of proteins, J. Bacteriol. 184 (2002) 629–635.

[9] F.W. Studier, A.H. Rosenberg, J.J. Dunn, J.W. Dubendorff, Use of T7 RNA polymerase to direct expression of cloned genes, Methods Enzymol. 185 (1990) 60–89.

[10] H. Schägger, G. von Jagow, Tricine–sodium dodecyl sulfate–polyacrylamide gel electrophoresis for the separation of proteins in the range from 1 to 100 kDa, Anal. Biochem. 166 (1987) 368–379.

[11] M.M. Carrió, A. Villaverde, Construction and deconstruction of bacterial inclusion bodies, J. Biotechnol. 96 (2002) 3–12.

[12] H. Wang, S. Chong, Visualization of coupled protein folding and binding in bacteria and purification of the heteromeric complex, Proc. Natl. Acad. Sci. USA 100 (2003) 478–483.

[13] N. Kholod, T. Mustelin, Novel vectors for co-expression of two proteins in *E. coli*, BioTechniques 31 (2001) 322–328.

[14] W. Yang, L. Zhang, Z. Lu, W. Tao, Z. Zhai, A new method for protein coexpression in *Escherichia coli* using two incompatible plasmids, Protein Express. Purif. 22 (2001) 472–478.

Interaction between the bacterial nucleoid associated proteins Hha and H-NS involves a conformational change of Hha

Jesús GARCÍA*, Tiago N. CORDEIRO*, José M. NIETO†, Ignacio PONS†, Antonio JUÁREZ†[1] and Miquel PONS*‡[1]

*Laboratory of Biomolecular NMR, Parc Científic de Barcelona, Josep Samitier, 1-5, 08028-Barcelona, Spain, †Departament de Microbiologia, Universitat de Barcelona, Martí i Franquès, 1-11, 08028-Barcelona, Spain, and ‡Departament de Química Orgànica, Universitat de Barcelona, Martí i Franquès, 1-11, 08028-Barcelona, Spain

The H-NS family of proteins has been shown to participate in the regulation of a large number of genes in Gram-negative bacteria in response to environmental factors. In recent years, it has become apparent that proteins of the Hha family are essential elements for H-NS-regulated gene expression. Hha has been shown to bind H-NS, although the details for this interaction are still unknown. In the present paper, we report fluorescence anisotropy and NMR studies of the interaction between Hha and H-NS_{64}, a truncated form of H-NS containing only its N-terminal dimerization domain. We demonstrate the initial formation of a complex between one Hha and two H-NS_{64} monomers in 150 mM NaCl. This complex seems to act as a nucleation unit for higher-molecular-mass complexes. NMR studies suggest that Hha is in equilibrium between two different conformations, one of which is stabilized by binding to H-NS_{64}. A similar exchange is also observed for Hha in the absence of H-NS when temperature is increased to 37 °C, suggesting a key role for intrinsic conformational changes of Hha in modulating its interaction with H-NS.

Key words: fluorescence anisotropy, Hha, H-NS, NMR, nucleoid-associated protein, protein–protein interaction.

INTRODUCTION

Bacterial nucleoid-associated proteins play both structural and modulatory roles. In Gram-negative bacteria, the H-NS family of proteins has deserved extensive research efforts [1]. Proteins belonging to this family are involved in organizing the nucleoid structurally and in the regulation of the expression of many operons (for recent reviews, see [2–4]). Among others, environmental factors such as osmolarity or temperature [5,6] switch regulatory responses requiring the presence of H-NS. In *Escherichia coli*, up to 5 % of the genes are subjected to H-NS modulation [7]. H-NS proteins do not exhibit a preference for specific DNA sequences, but rather for DNA structures: curved DNA sequences are usually targets for H-NS [8]. To repress transcription, binding to two distant sites located nearby the promoter, H-NS oligomerization and nucleation of the DNA region appear as key steps [9–11]. Nevertheless, the specific molecular details of the process remain to be elucidated.

In recent years, there has been evidence that at least some of the processes that require H-NS to modulate gene expression may require H-NS to interact directly with other proteins. Generation of heterodimers between H-NS and its paralogue StpA has been reported [12–14]. Interaction of H-NS with StpA protects StpA from Lon-mediated proteolysis [13]. It has also been shown that StpA can act as a molecular adapter for some species of truncated H-NS proteins to repress the *bgl* operon [15]. However, details of the modulatory role of such heterodimers remain to be elucidated.

Characterization of the Hha/YmoA family of nucleoid-associated proteins has also provided evidence for protein–protein interactions underlying H-NS-mediated modulation of gene expression. Proteins of the Hha/YmoA family are small (approx. 8 kDa) and are moderately basic. They were reported to repress gene expression in different enterobacteria in response to changes in temperature or osmolarity [16,17]. When analysing sequence similarity data, no apparent relationship with other families of nucleoid-associated proteins could be established. Studies focused to understand the mechanism underlying Hha-mediated repression of *E. coli* toxin α-haemolysin showed that, rather than exhibiting DNA-binding activity, Hha exhibited H-NS-binding activity [18]. A role for a Hha–H-NS complex repressing the *hly* operon at low temperature was then shown [11,18]. Since then, interactions of other members of the family (YmoA, YdgT) with members of the H-NS family have also been shown [19,20]. In spite of the genetic and biochemical evidence demonstrating protein–protein interactions between both families of proteins, molecular details of the process are lacking. A mutational analysis of the Hha protein failed to identify a specific region of Hha involved in binding to H-NS. Instead, mutations in different regions can inhibit Hha binding to H-NS, suggesting that most of the protein is involved directly or indirectly in the binding process [19].

H-NS consists of an N-terminal dimerization domain and a C-terminal DNA-binding domain separated by a linker domain that is involved in the formation of high-molecular-mass oligomers [4]. A truncated form of H-NS comprising residues 1–64 (H-NS_{64}) has been reported to form only dimers [21]. An alignment of the amino acid sequences of members of the Hha family of proteins with the N-terminal region of H-NS-like proteins showed groups of conserved residues, which suggests that Hha-like proteins may be functionally equivalent to the N-terminal domain of H-NS-like proteins [19].

In the present paper, we report fluorescence anisotropy and NMR studies of the interaction between Hha and H-NS_{64} that allow the determination of the stoichiometry and stability of the complex formed and provide evidence for a conformational process in Hha associated with its interaction with H-NS_{64}, but that can be detected also in free Hha.

Abbreviations used: CPMG, Carr–Purcell–Meiboom–Gill; DTT, dithiothreitol; HSQC, heteronuclear single-quantum correlation NMR spectroscopy; IPTG, isopropyl β-D-thiogalactoside; Ni-NTA, Ni^{2+}-nitrilotriacetate.

[1] Correspondence can be addressed to either of these authors (email mpons@ub.edu or ajuarez@ub.edu).

MATERIALS AND METHODS

DNA clones

The clone encoding His_6–Hha has been described previously [22]. The expressed sequence is MGSS$(H)_6$SSGRENLYFQGH-(Hha)GS. H-NS_{64}, carrying a C-terminal His_6-purification tag, was prepared by PCR amplification from a full-length *E. coli* H-NS plasmid [19]. Restriction sites, His_6-tag and a C-terminal stop codon were introduced using PCR primers: sense primer, 5′-GATTACTACCATGGGCGAAGC-3′ and antisense primer, 5′-CGGGATCCTATTAATGGTGATGGTGATGGTGCAGCATTTCGCGA-3′ (restriction sites are underlined). The PCR product was then subcloned into the NcoI/BamHI sites of plasmid pET-15b (Novagen) following standard protocols. All clones were sequenced before use.

Protein expression and purification

Transformed BL21(DE3) cells were grown at 37 °C in either LB (Luria–Bertani) or in M9 minimal medium containing $^{15}NH_4Cl$ until a D_{600} of 0.7 was reached. In both cases, Hha overexpression was induced overnight at 15 °C by the addition of IPTG (isopropyl β-D-thiogalactoside) (1 mM final concentration). Cell pellets were frozen, resuspended in 20 mM Tris/HCl, 800 mM NaCl, 15 mM 2-mercaptoethanol and 5 mM imidazole, pH 8.0, and lysed by sonication (six 10 s pulses). The lysate was centrifuged at 20 000 ***g*** for 30 min at 4 °C, and the supernatant was then treated with Ni-NTA (Ni^{2+}-nitrilotriacetate)–agarose (Qiagen). The resin was washed extensively with the same buffer, and the protein was eluted using 400 mM imidazole. A final purification step on a Superdex 75 column in 20 mM sodium phosphate, 150 mM NaCl, 2 mM DTT (dithiothreitol) and 0.01 % (w/v) sodium azide, pH 7.0, yielded pure Hha as a monomer. MS of the purified protein gave a molecular mass of 11 202 Da, corresponding to the sequence expressed with the depletion of the N-terminal methionine residue. Oligomers were occasionally formed during purification or upon storage, but were cleanly separated by size-exclusion chromatography on a Superdex 75 column. The purity and aggregation state of Hha was checked by gel filtration, SDS/PAGE, MS and steady-state fluorescence anisotropy.

H-NS_{64} was expressed using the same procedure, except that expression was initiated with 0.5 mM IPTG, lysis and purification steps were carried out in the presence of 1 M NaCl, 20 mM 2-mercaptoethanol and 0.5 mM EDTA, and the protein was eluted from the Ni-NTA resin with 50 mM EDTA. Ni-EDTA was removed by gel filtration on a Superdex 75 column. Compared with protein molecular-mass standards, H-NS_{64} showed an apparent molecular mass consistent with a dimer. MS gave the expected mass for H-NS_{64} monomer. Ellman analysis, after dialysis to remove DTT, confirmed that cysteine was in the reduced form.

Fluorescence spectroscopy

In contrast with full-length H-NS, H-NS_{64} does not contain tryptophan, allowing for selective observation of Hha fluorescence during complex formation.

Hha samples used for fluorescence measurements were prepared directly from the isolated peak corresponding to the Hha monomer from a Superdex 75 column, quantified using the absorption intensity at 280 nm and diluted to the desired concentration. Samples stored for more than 1 week and showing higher anisotropy than expected were re-purified before use.

Fluorescence measurements were performed in 20 mM sodium phosphate, pH 7.0, 150 mM NaCl, 0.01 % (w/v) sodium azide and 1 mM Tris(2-carboxyethyl)phosphine. This reducing agent was used in order to minimize both the absorption and the fluorescence background.

Fluorescence spectra were recorded in 1 cm path-length cells at 25 °C on an Aminco Bowman AB2 fluorimeter using an excitation wavelength of 295 nm to minimize excitation of tyrosine and an excitation bandwidth of 2 nm. Emission spectra were obtained as the ratio between observed and reference signals, and were corrected for instrument response and background fluorescence. Relative quantum yields of Hha or Hha–H-NS_{64} complexes were obtained by comparing the integrated intensities of their fluorescence spectra with those of tryptophan measured in the same buffer (i.e. with the same refractive index) and the same total absorption. The ratios of quantum yields of Hha and tryptophan in one hand, and complexed and free Hha in the other, are both 0.95. The sample of complexed Hha is a 1:2.5 mixture with H-NS_{64}. The absorbance of the samples was kept below 0.05 absorbance units to avoid inner filter effects.

Fluorescence anisotropy

Steady-state fluorescence anisotropy is observed after excitation with polarized light if the correlation time for the re-orientation of the chromophore is long with respect to the fluorescence lifetime. Steady-state anisotropy is related to correlation time of an isotropic species through the Perrin equation (eqn 1) [23]:

$$\frac{1}{A} = \frac{1}{A_0}\left(1 + \frac{\zeta}{\tau}\right) \quad (1)$$

where A_0 is the anisotropy expected for a fixed macromolecule and includes intrinsic factors of the chromophore and local motion effects, ζ is the fluorescence lifetime, and τ is the isotropic rotational correlation time. Fluorescence anisotropy can be used to follow the increase in correlation time associated with the formation of protein–protein complexes.

Steady-state fluorescence anisotropy was determined at 344 nm with a bandwidth of 4 nm using an autopolarizer accessory with 'L' geometry, and is the average of 40 measurements, each with an independent determination of the G-factor. Experimental uncertainty was evaluated by comparing at least three duplicates of the complete measurement and was ± 0.001.

The correlation time of Hha in complexes can be estimated from the ratio of fluorescence anisotropies of free and complexed Hha using eqn (2), which is directly derived from eqn (1):

$$\tau_b = \frac{R\tau_f\zeta_b}{\tau_f(1-R) + \zeta_f} \quad (2)$$

where $R = A_b/A_f$, τ_b and τ_f are isotropic correlation times of the free and bound forms, and ζ_f and ζ_b are the corresponding fluorescence lifetimes.

The implicit assumption that A_0 in Perrin's equation is not significantly affected by complexation is supported by the similar emission maxima and quantum yields.

The correlation time for free Hha at 25 °C was estimated using the Stokes–Einstein equation [23] and the molecular mass of Hha. The fluorescence lifetimes were obtained from the relative quantum yields measured for tryptophan, free Hha and Hha in the presence of 2.5 equivalents of H-NS_{64}. Taking as a reference the lifetime of tryptophan (2.6 ns at pH 7.0 and 25 °C) the lifetimes of tryptophan in Hha and Hha–H-NS_{64} complexes were calculated to be 2.47 and 2.35 ns respectively under our experimental conditions.

The fluorescence anisotropy of the complex was obtained from the fitting of a titration of Hha with H-NS_{64} (see below).

H-NS$_{64}$ titrations

H-NS$_{64}$ titrations were carried out at 25 °C with freshly purified Hha and H-NS$_{64}$ samples. The sample initially contained 2 ml of 4 μM Hha, and, for each point, 70 μl of a H-NS$_{64}$ stock solution was added and incubated for 5 min with magnetic stirring before measurement. The accuracy of the volumes added was calibrated gravimetrically and was better than ± 0.2 μl. The actual concentrations, corrected for the effects of dilution at each point, were used for the analysis. Titration curves were analysed using a model involving the formation of a 1:2 complex:

$$\text{Hha} + 2\text{H-NS}_{64} \rightleftharpoons \text{Hha} - (\text{H-NS}_{64})_2$$

with a dissociation constant, K_d, given by

$$K_d = \frac{[\text{Hha}][\text{H-NS}_{64}]^2}{[\text{Hha} - (\text{H-NS}_{64})_2]} \quad (3)$$

The fraction of Hha bound to H-NS$_{64}$ can be determined from the fluorescence anisotropy, corrected by the relative quantum yields of Hha in the free (Φ_f) and bound (Φ_b) forms using eqn (4) [24].

$$f_b = \frac{A - A_f}{A_b - A + Q(A - A_f)} \quad (4)$$

where A is the observed anisotropy and A_f and A_b are the anisotropies of free Hha and the complex respectively and $Q = \Phi_b/\Phi_f$.

By combining eqns (3) and (4), the observed anisotropy A can be related to the known values of A_f, Q and the total concentrations of Hha and H-NS$_{64}$, and the unknown parameters: K_d and A_b. These were determined by non-linear minimization of the error function

$$\chi^2 = \sum \frac{(A_{obs} - A_{th})^2}{\sigma^2} \quad (5)$$

where A_{obs} is the observed fluorescence anisotropy, A_{th} is the value predicted by the model and σ^2 is the experimental uncertainty. The minimization was carried out using in-house scripts written in Mathematica (Wolfram Research). Alternative models, including the formation of an intermediate 1:1 complex, were compared using the fitting and statistical tools of DynaFit, without the inclusion of quantum yield corrections [25]. Alternative models were compared using F-statistics. Error estimates were obtained from DynaFit.

NMR spectroscopy

NMR samples used for variable temperature spectra and for titrations with H-NS$_{64}$ were 80–90 μM uniformly ^{15}N-labelled Hha in 20 mM sodium phosphate buffer, 150 mM NaCl, 2 mM DTT and 0.01 % (w/v) sodium azide, pH 7.0, in the presence of 10 % (v/v) ^2H_2O. ^{1}H-^{15}N HSQC (heteronuclear single-quantum correlation NMR spectroscopy) spectra were recorded on a Bruker Avance 600 using 1024 × 128 points and 48 accumulations. Assignments of ^{1}H-^{15}N HSQC spectra at 25 °C were obtained from Yee et al. [22].

^{1}H-^{15}N HSQC experiments containing a relaxation compensated CPMG (Carr–Purcell–Meiboom–Gill) filter [26] were recorded at 37 °C on a Bruker Avance 800 MHz. Two experiments with an identical duration of the CPMG train (32 ms), but with different CPMG refocusing delays (250 and 500 μs), were collected.

Temperature coefficients ($\delta\Delta_{NH}/\Delta T$) in parts per billion per K, where $\delta\Delta_{NH}$ is the difference of the HN chemical shift, were measured from a series of four ^{1}H-^{15}N HSQC experiments recorded between 25 and 37 °C, and were obtained by plotting the amide chemical shift versus the temperature. Chemical-shift values were referenced considering the temperature-dependence of HDO chemical shifts [27].

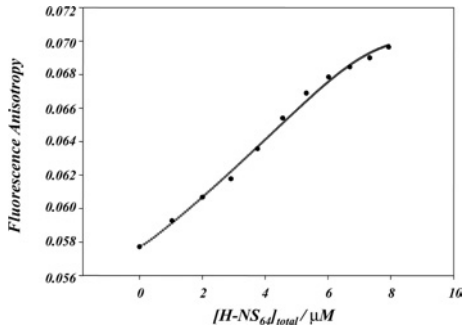

Figure 1 Fluorescence anisotropy titration of Hha with H-NS$_{64}$

Titration was carried out at 25 °C with an initial Hha concentration of 4 μM.

CD

CD spectra were measured on a JASCO J-810 instrument, equipped with a Peltier accessory for temperature control, using a 1 cm path-length cell. CD measurements were performed at far UV (200–250 nm) with a scan speed of 50 nm/min, 4 nm bandwidth and an average response time of 4 s.

RESULTS

Fluorescence anisotropy provides the stoichiometry of the complex and its dissociation constant

H-NS$_{64}$ has no tryptophan residues and it is therefore possible to observe the formation of Hha–H-NS$_{64}$ complexes using the intrinsic fluorescence of Hha. Emission spectra of Hha were measured with excitation at 295 nm to minimize light absorption by tyrosine. The emission maximum at 25 °C is at 344 nm, typical of a partially solvent exposed tryptophan side chain. In the presence of 2.5 equivalents of H-NS$_{64}$, the emission maximum is shifted to 340 nm.

Figure 1 shows the change in fluorescence anisotropy of Hha caused by the addition of H-NS$_{64}$. The fluorescence anisotropy of Hha increases and levels off after the addition of approx. 2 equivalents of H-NS$_{64}$ to Hha, suggesting the formation of a discrete complex. A good fitting of the curve was achieved assuming the formation of a 1:2 complex with a dissociation constant of 0.45 μM^2 at 25 °C in 20 mM sodium phosphate buffer and 150 mM NaCl, pH 7.0. The uncertainty estimated from the fitting was ± 0.08. The actual precision could be lower, as the concentration of free H-NS$_{64}$ was determined indirectly in an iterative procedure.

Small deviations between computed and experimental curves are not due to interference from intrinsic monomer–dimer equilibria for H-NS$_{64}$. In gel-filtration experiments in the absence of Hha, H-NS$_{64}$ elutes at a constant volume, consistent with the molecular mass of a dimer, at concentrations between 4 and 470 μM (T. N. Cordeiro and J. Garcia, unpublished work). A truncated form of H-NS containing only the first 46 residues forms dimers with a dissociation constant lower than 5 nM, as determined by fluorescence anisotropy [28]. Dissociation of H-NS$_{64}$ dimers induced by Hha cannot be ruled out. A model assuming an intermediate 1:1 species is compatible with titration data and gives a lower χ^2. However, the fitting requires two additional adjustable

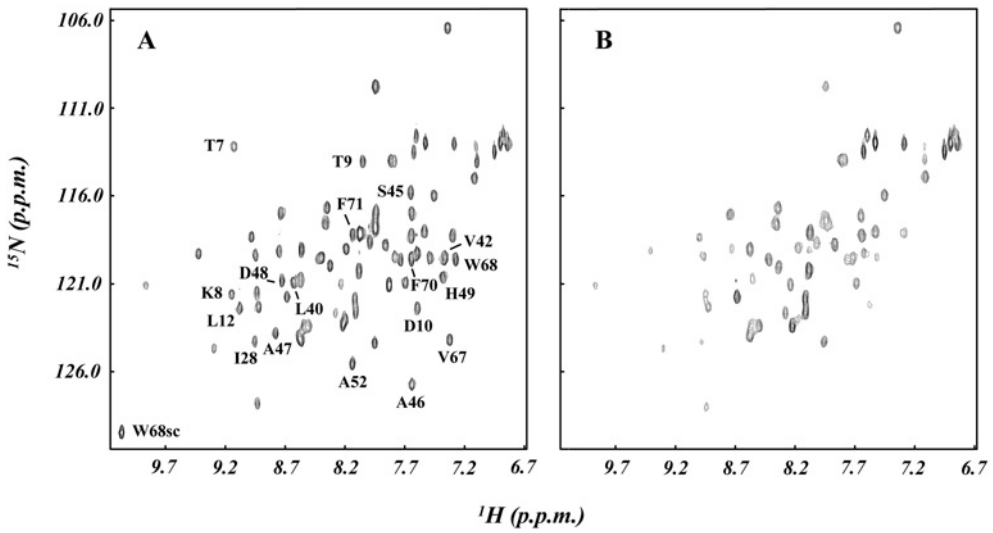

Figure 2 ^{1}H-^{15}N HSQC spectra of Hha in the presence or the absence of H-NS$_{64}$

(**A**) ^{1}H-^{15}N HSQC spectrum of 90 μM uniformly ^{15}N-labelled Hha at 25 °C under the conditions described in the Materials and methods section. (**B**) ^{1}H-^{15}N HSQC spectrum under the same conditions after addition of 45 μM unlabelled H-NS$_{64}$. Broadening causes a decrease in intensity of signals. Cross-peak intensities were normalized with respect to the one showing the highest intensity in each spectrum. Residues that show a decrease in normalized intensity below 25 % of the value observed in free Hha are labelled. Side-chain NH groups are indicated by 'sc' after the residue number.

parameters (two binding constants and two anisotropy values). A comparison of the 1:2 and 1:1 models gives an F value of 2.17, which is lower than the limit value of 2.72 (90 % confidence, and 9 and 7 degrees of freedom). One should conclude that the 1:1 model, although it cannot be excluded, does not provide a statistically significant improvement in the explanation of the present experimental data.

The anisotropy derived from the fitting provides an estimation of the correlation time of the complex which depends strongly on the reference correlation time assumed for free Hha. Reference values of 4 and 5 ns provide estimates of 7.6 and 11.0 ns for the correlation time of the complex using eqn (2). The correlation time calculated for a sphere with a mass corresponding to the molecular mass of the Hha–(H-NS$_{64}$)$_2$ complex is 10.1 ns.

Addition of excess H-NS$_{64}$ causes a marked increase in fluorescence anisotropy, indicating that higher-molecular-mass species containing Hha are being formed (results not shown). In the presence of more than 2.5 equivalents (8 μM) of H-NS$_{64}$, species with longer correlation times containing Hha are formed. In the absence of Hha, H-NS$_{64}$ forms only dimers even at much higher concentrations. High-molecular-mass Hha$_m$–(H-NS$_{64}$)$_n$ (where m and n are variables) hetero-oligomers are thus induced by the presence of Hha, probably by the addition of further H-NS$_{64}$ molecules to the initially formed Hha–(H-NS$_{64}$)$_2$ complex.

Titration with H-NS$_{64}$ affects residues in the hydrophobic core of Hha

The three-dimensional structure of Hha at 25 °C has been solved by NMR [22]. The structure of Hha consists of four α-helical segments: helix 1 (residues 8–16), helix 2 (residues 21–34), helix 3 (residues 37–55) and helix 4 (residues 65–70). The four helical segments are separated by loops. The architecture of Hha is constructed around the long helix 3. Helices 1 and 2 are packed against the N-terminal half of helix 3. Helix 4 is very short and interacts with the C-terminal part of helix 3.

^{15}N-labelled Hha gives sharp well-resolved HSQC spectra at 25 °C. In the presence of 1 equivalent of H-NS$_{64}$, severe broadening of Hha signals is observed at 25 °C, leading to a general decrease in intensity of the whole spectra (results not shown). However, when only a 0.5 equivalent of H-NS$_{64}$ is added, most of the signals are still visible, but differential broadening of a set of residues is clearly observed. Figure 2 shows HSQC spectra of 90 μM ^{15}N-labelled Hha before and after the addition of 0.5 equivalents of unlabelled H-NS$_{64}$.

The broadening observed at 25 °C results from exchange between two sites in the intermediate regime, i.e. at a rate comparable with the difference in the chemical-shift frequencies of the two sites. This is clearly demonstrated by lowering the temperature to 7 °C. At this temperature, the rate of exchange becomes lower than the frequency difference, and duplicate signals are observed for the free and bound forms. Figure 3 shows an expansion of signals from Ala^{46} of Hha in a series of HSQC spectra measured at 7 °C in the presence of increasing amounts of H-NS$_{64}$. A decrease of signals from free Hha and an increase in the intensity of a new signal corresponding to the formation of a complex are clearly observed.

Exchange broadening depends on the exchange rate, the frequency difference between exchanging sites and the product of the relative populations of the sites. At low concentrations of H-NS$_{64}$, only those residues showing the largest frequency differences between exchanging sites show extensive broadening. Figure 4 shows the location of affected residues in the structure of Hha. Residues whose NH signals are most perturbed by the addition of H-NS$_{64}$ are located in the four helices of Hha: residues Lys^8, Thr^9, Asp^{10} and Leu^{12} are at the N-terminus of helix 1. Helix 3 has eight residues perturbed by H-NS$_{64}$: Leu^{40}, Val^{42}, Ser^{45}, Ala^{46}, Ala^{47}, Asp^{48}, His^{49} and Ala^{52}. Five of them, i.e. more than one complete helix turn, are consecutive (Ser^{45}–His^{49}). Val^{42}, Ser^{45}, Ala^{46}, His^{49} and Ala^{52} are on one side of the helix, and Ala^{46} is at the interface between helices 1 and 3. Leu^{40} and Ala^{47} are in the opposite side of helix 3, and are flanking two aromatic residues (Phe^{43} and Tyr^{44}) that form the interface with helix 2. Helix 4 has three residues broadened by the addition of H-NS$_{64}$: Val^{67}, Trp^{68} and Phe^{70}. Ile^{28} is the only perturbed residue in helix 2 and is located at the contact interface with helix 3.

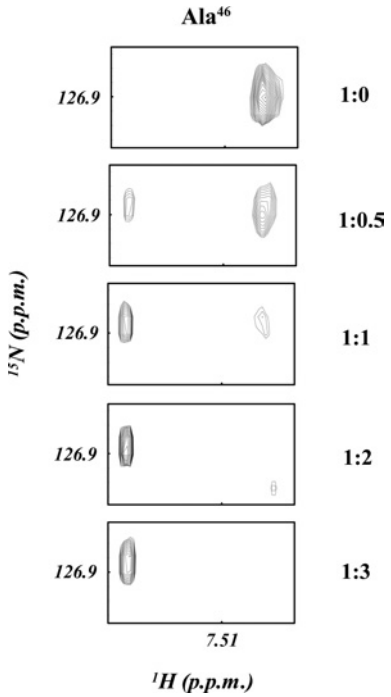

Figure 3 ^{1}H-^{15}N HSQC spectra at 7 °C of Hha with increasing amounts of H-NS$_{64}$

Expansions of the ^{1}H-^{15}N HSQC spectra recorded at 7 °C illustrating the decrease in intensity of the Ala^{46} cross-peak in the presence of increasing concentrations of H-NS$_{64}$. A new peak corresponding to the complex appears simultaneously. The Hha/H-NS$_{64}$ ratio is indicated on the right.

Temperature effects on Hha conformation

Exchange effects observed in core residues of Hha when it binds to H-NS$_{64}$ suggest that Hha changes its conformation, and we have tried to determine whether, in the absence of H-NS$_{64}$, alternative conformations of Hha are also accessible. The presence of exchange in free Hha could be revealed by non-linear changes in chemical shifts or by the observation of exchange-broadening effects similar to those observed in the presence of H-NS$_{64}$ induced by a small temperature increase.

Figure 5 shows a comparison of ^{1}H-^{15}N-HSQC spectra of 80 μM Hha at 25 and 37 °C. In spite of the lower correlation time at higher temperatures that is expected to give narrower NMR line widths, at 37 °C, exchange broadening is observed for all residues, but is especially significant for six residues which show intensity below 25 % of that observed at 25 °C: Lys^{8}, Ile^{21}, Ile^{28}, Tyr^{44}, Tyr^{60} and Ile^{63}. An exchange contribution to most of the NH peaks could be confirmed by comparing the intensities of ^{1}H-^{15}N HSQC spectra filtered with relaxation-compensated CPMG periods of identical duration, but differing in the interpulse delay (Figure 6). Exchange effects are minimized when interpulse delays are shorter and signal intensity in these spectra will be higher.

Temperature coefficients represent the dependence of chemical shift on temperature. In rigidly structured proteins, amide protons usually show negative temperature coefficients with values that depend on solvent exposure or hydrogen bond formation. Positive temperature coefficients are usually indicative of conformational exchange [29]. Four Hha residues show positive temperature coefficients in their amide proton signals (Figure 6): Ala^{41}, Ala^{46}, Val^{67} and Trp^{68}. In addition, Val^{67} changes its ^{15}N chemical shift between 25 and 37 °C. The aliphatic region of ^{1}H-NMR spectra obtained at 25 and 37 °C also present frequency shifts and variations

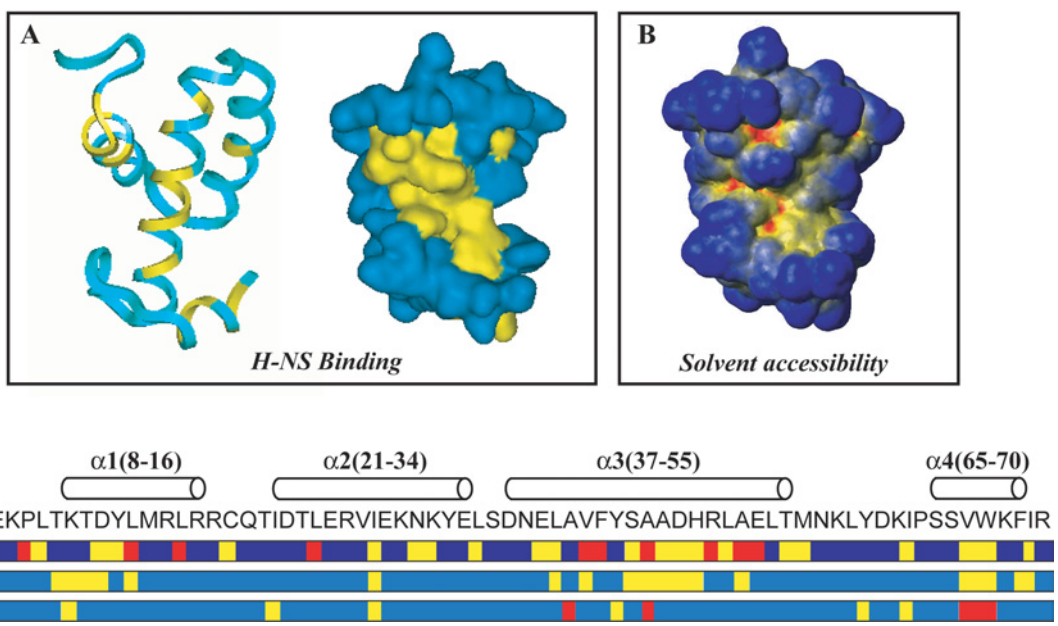

Figure 4 Overview of Hha residues affected by H-NS$_{64}$ binding and temperature changes

(**A**) Ribbon and surface representation of Hha structure. Residues most affected by broadening in the presence of a 0.5 equivalent of H-NS$_{64}$ are coloured yellow. The affected residues are identified along the sequence in (**C**, row 4). (**B**) Solvent accessibility of Hha. Residues are coloured according to the percentage of solvent-exposed surface: red (< 5 %), yellow (5–20 %) and blue (> 20 %). The sequence location of buried residues is indicated in (**C**, row 3) using the same colour code. (**C**) Secondary structure (row 1), solvent exposure (row 3), H-NS$_{64}$-induced perturbations (row 4) and temperature-induced exchange effects (row 5) are compared along the Hha sequence (row 2). In row 5, residues that are selectively broadened at 37 °C are indicated in yellow and those whose temperature coefficients are positive in red.

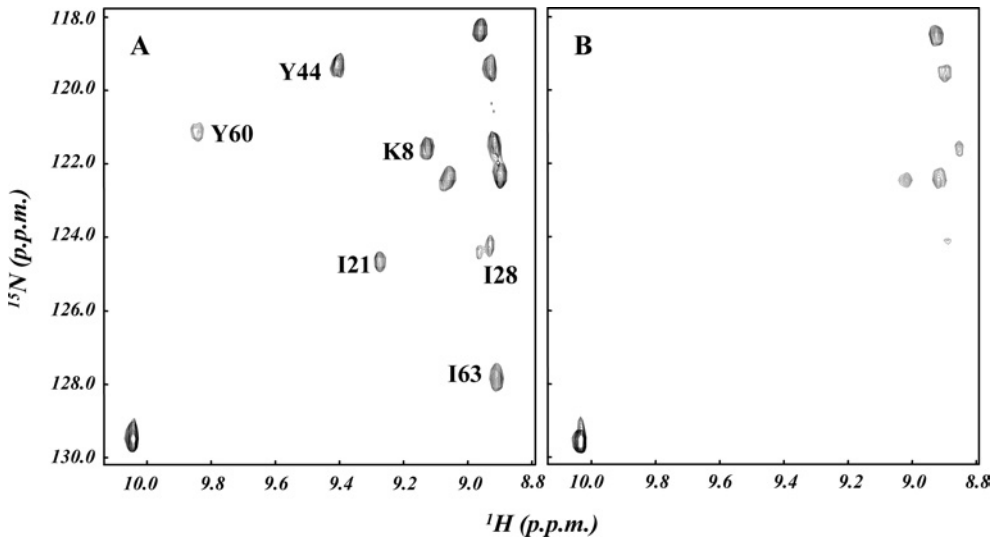

Figure 5 Comparison of ^{1}H-^{15}N HSQC spectra of Hha at 25 °C and 37 °C

^{1}H-^{15}N HSQC expansions of Hha (80 μM) under analogous conditions to those described in the Materials and methods section recorded at 25 °C (**A**) or 37 °C (**B**). Exchange between different conformations causes variations in line width of most of the cross-peaks. Residues that show the largest effects have been labelled.

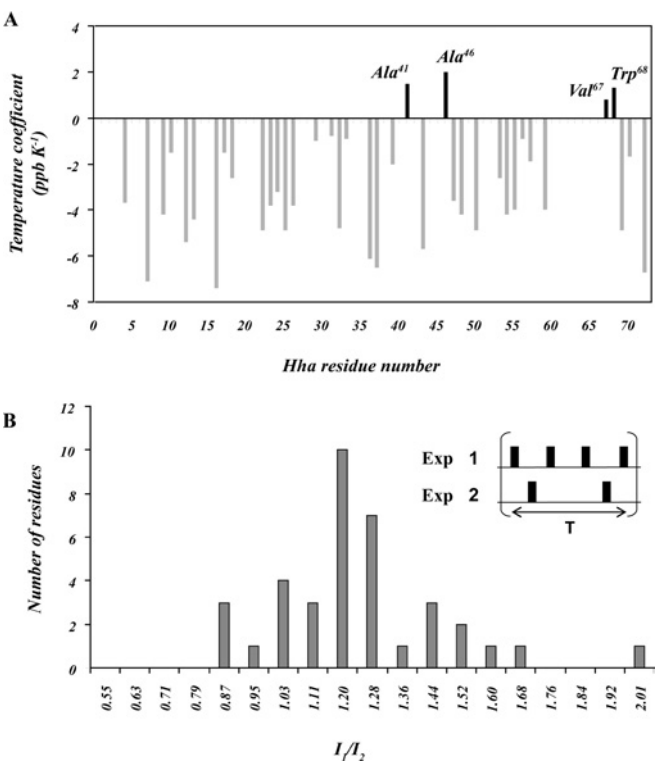

Figure 6 NMR evidence for temperature-induced conformational exchange in Hha

(**A**) Temperature coefficients of NH signals of Hha. Residues showing positive temperature coefficients, indicative of exchange, are highlighted. (**B**) Distribution of intensity ratios between equivalent cross-peaks in two CPMG-filtered HSQC experiments with 250 (exp 1) and 500 μs (exp 2) interpulse delays, but identical CPMG length. Ratios (exp 1/exp 2) higher than 1 are indicative of chemical exchange. The higher sensitivity of CPMG experiments show that exchange affects most residues of Hha, as expected for a global conformational change. The temperature was 37 °C, and only well-resolved signals visible at this temperature are included.

in line width, suggesting exchange between different conformations (results not shown). All changes are reversible.

We have used CD to determine the effect of temperature in the secondary structure of Hha. CD spectra of Hha (results not shown) are typical for a helical protein, with minima at 205 and 222 nm. The change in elipticity between 6 °C and 40 °C is linear. The elipticity at 222 nm measured at 37 °C is 96 % of the value observed at 25 °C, and the change is fully reversible. Therefore the secondary structure of Hha is not substantially affected by the increase in temperature from 25 to 37 °C. These results suggest that temperature-induced changes in Hha correspond to a change in tertiary structure leading to a modification of helical packing.

DISCUSSION

Hha is known to bind to H-NS, and the presence of Hha affects the expression of genes under H-NS control. Although the overall homology between Hha and H-NS is low, Hha shows groups of conserved residues with the dimerization domain of H-NS present in a truncated form containing only the first 64 residues of H-NS. Our fluorescence and NMR results clearly show that Hha interacts strongly with the dimerization domain of H-NS. The stoichiometry of the complex formed under the experimental conditions used in the present study (20 mM sodium phosphate and 150 mM NaCl, pH 7.0, 25 °C) suggests that Hha interacts with two H-NS$_{64}$ molecules.

The interaction between Hha and H-NS$_{64}$ causes important changes in the NMR spectra of Hha that affect residues that are solvent-accessible in the published three-dimensional structure [22], as well as some deeply buried residues including residues located in the interface between helices 1, 2 and 3 in Hha.

At 25 °C, conformational-complexation-induced exchange causes broadening of a number of residues. At 7 °C, the rate of exchange is reduced and separate signals are observed for free and bound forms. The relative intensities change by the addition of H-NS$_{64}$ and, in the presence of approx. 2 equivalents of H-NS$_{64}$, only signals from the complex are observed, in agreement with

the stoichiometry determined from fluorescence results. However, under our present experimental conditions, the sensitivity is still too low to attempt the complete determination of the structure of the complex.

Perturbed residues include both surface and buried residues. While surface residues could be directly in contact with H-NS_{64}, perturbation of buried residues suggests a major conformational rearrangement induced by complexation. Some of the perturbed residues are completely buried in the hydrophobic core of Hha with a very low percentage of its surface exposed to solvent (Figure 4). Some of these residues are located at the interface between helices: Ala^{46} (0.1 % accessibility) between helices 1 and 3, and Ile^{28} (accessibility 13.6 %) between helices 2 and 3. This observation indicates that Hha experiences a conformational change upon complexation and suggests a model in which Hha may exist in a 'closed' form, corresponding to the structure determined by NMR for the isolated molecule, and an 'open' form that is stabilized by interaction with H-NS_{64}.

Conformational plasticity is present in Hha, even in the absence of H-NS_{64}. Major changes in line widths and chemical shifts are observed when the temperature is increased from 25 to 37 °C. At 37 °C, the exchange rate and, probably, the relative populations of the closed and open conformations change, leading to the observed broadening and chemical-shift effects. Figure 4 shows that residues that are affected by changes in temperature and by the addition of H-NS_{64} at 25 °C partially overlap. In particular, residues Ala^{46} and Ile^{28} located at helix interfaces are perturbed both by H-NS_{64} binding and by temperature perturbation. Ile^{28} is the only perturbed residue of helix 2 and provides an example of a residue that is probably affected mainly by conformational effects, but is not interacting directly with H-NS_{64}. CD spectra are nearly unaffected by changing the temperature from 25 to 37 °C, indicating that the helix content does not change significantly between the two temperatures. The observed conformational change therefore seems to imply a change in the helix packing of Hha. A similar effect has been observed for the apo regulatory domain of skeletal muscle troponin C [30].

Interaction with H-NS_{64} causes a stabilization of the open form. H-NS_{64}-induced broadening observed at 25 °C may contain a contribution from exchange between free and complexed forms, as well as exchange between open and closed conformation that are still possible in the complex. At 25 °C, broadening is still observed in the presence of 3 equivalents of H-NS_{64}. This suggests that the observed broadening is not just the result of the equilibration between free and bound species. Further work is still needed to separate both possibilities.

A similar effect has been reported for calmodulin. The N-terminal domain of calmodulin is in equilibrium between an open and a closed form that is modulated by calcium complexation [31]. In the apo-form, the interaction with a target peptide causes broadening of a number of residues that are not concentrated in a discrete binding interface and has been interpreted as a modulation of the equilibrium between open and closed forms by the peptide [32].

Our NMR results show that Hha experiences a conformational change, affecting the packing of the helices, when it binds to H-NS_{64}. A similar conformational equilibrium takes place in free Hha and is strongly affected by changing the temperature from 25 to 37 °C. It is suggestive that temperature acts as a signal for bacterial colonization of warm-blooded hosts, and the temperature sensor involved should be sensitive to changes in temperature from a lower ambient temperature to 37 °C. It is now well-established that the H-NS system is involved in mediating changes in gene expression regulated by temperature [5,6]. The conformational equilibrium of Hha may provide a sensor mechanism for modulating H-NS-regulated gene expression in response to environmental changes such as temperature and osmolarity.

Fluorescence anisotropy demonstrates the formation of additional Hha species with longer correlation times in the presence of excess H-NS_{64}. This can be interpreted as an indication that Hha can also nucleate the formation of hetero-oligomers of H-NS_{64} under experimental conditions in which H-NS_{64} only forms dimers. The observed 1:2 complex is probably a first step in this nucleation. These results are consistent with the fact that, in the presence of Hha, complexes between full-length H-NS and its target DNA sequences in the operon encoding for the toxin α-haemolysin, migrate slower than those obtained in the absence of Hha [18] suggesting the formation of Hha_m–$(H\text{-}NS_{64})_n$ hetero-oligomers of molecular mass higher that those generated by H-NS alone.

The H-NS system is composed of H-NS itself, which is able to interact with DNA and to oligomerize the DNA regions where H-NS interacts, which may have characteristic bending capabilities, and H-NS-binding proteins that modulate H-NS's ability to oligomerize. Our results lend support to the role of Hha as a modulator of H-NS oligomerization and identify the N-terminal domain of H-NS as an interaction site. Our results also suggest a possible mechanism by which environmental changes affecting conformational equilibria in Hha may cause changes in the expression of genes under H-NS control. Our groups are actively pursuing this line of research.

We thank C. Arrowsmith and A. Yee for providing the clone of Hha used in this study, and O. Millet for helpful discussions and assistance in the recording of relaxation-compensated CPMG experiments. J. G. acknowledges support from MCyT Ramon y Cajal program. The project was partially supported by funds from MCyT (BIO2001-3115, BIO2004-5436 to M. P., and BMC2001-3499, 2001SGR00100 to A. J.). NMR instrumentation is part of the SCT of the University of Barcelona. T. N. C. is an Erasmus-Socrates student from the Departamento de Engenharia Química, Instituto Superior Técnico, Lisboa, Portugal.

REFERENCES

1 Tendeng, C. and Bertin, P. N. (2003) H-NS in Gram-negative bacteria: a family of multifaceted proteins. Trends Microbiol. **11**, 511–518
2 Dorman, C. J. (2004) H-NS: a universal regulator for a dynamic genome. Nat. Rev. Microbiol. **2**, 391–400
3 Rimsky, S. (2004) Structure of the histone-like protein H-NS and its role in regulation and genome superstructure. Curr. Opin. Microbiol. **7**, 109–114
4 Schröder, O. and Wagner, R. (2002) The bacterial regulatory protein H-NS: a versatile modulator of nucleic acid structures. Biol. Chem. **383**, 945–960
5 Atlung, T. and Ingmer, H. (1997) H-NS: a modulator of environmentally regulated gene expression. Mol. Microbiol. **24**, 7–17
6 Hurme, R. and Rhen, M. (1998) Temperature sensing in bacterial gene regulation – what it all boils down to. Mol. Microbiol. **30**, 1–6
7 Hommais, F., Krin, E., Laurent-Winter, C., Soutourina, O., Malpertuy, A., Le Caer, J. P., Danchin, A. and Bertin, P. (2001) Large-scale monitoring of pleiotropic regulation of gene expression by the prokaryotic nucleoid-associated protein H-NS. Mol. Microbiol. **40**, 20–36
8 Yamada, H., Muramatsu, S. and Mizuno, T. (1990) An *Escherichia coli* protein that preferentially binds to sharply curved DNA. J. Biochem. **108**, 420–425
9 Spurio, R., Falconi, M., Brandi, A., Pon, C. L. and Gualerzi, C. O. (1997) The oligomeric structure of nucleoid protein H-NS is necessary for recognition of intrinsically curved DNA and for bending. EMBO J. **16**, 1795–1805
10 Falconi, M., Colonna, B., Prosseda, G., Micheli, G. and Gualerzi, C. O. (1998) Thermoregulation of *Shigella* and *Escherichia coli* EIEC pathogenicity: a temperature-dependent structural transition of DNA modulates accessibility of VirF promoter to transcriptional repressor H-NS. EMBO J. **17**, 7033–7043
11 Madrid, C., Nieto, J. M., Paytubi, S., Falconi, F., Gualerzi, C. O. and Juárez, A. (2002) Temperature- and H-NS-dependent regulation of a plasmid-encoded virulence operon expressing *Escherichia coli* hemolysin. J. Bacteriol. **184**, 5058–5066
12 Williams, R. M., Rimsky, S. and Buc, H. (1996) Probing the structure, function, and interactions of the *Escherichia coli* H-NS and StpA proteins by using dominant negative derivatives. J. Bacteriol. **178**, 4335–4343

13 Johansson, J. and Uhlin, B. E. (1999) Differential protease-mediated turnover of H-NS and StpA revealed by a mutation altering protein stability and stationary survival of *Escherichia coli*. Proc. Natl. Acad. Sci. U.S.A. **96**, 10776–10781
14 Johansson, J., Eriksson, S., Sondén, B., Wai, S. N. and Uhlin, B. E. (2001) Heteromeric interactions among nucleoid-associated bacterial proteins: localization of StpA stabilizing regions in H-NS of *Escherichia coli*. J. Bacteriol. **183**, 2343–2347
15 Free, A., Porter, M., Deighan, P. and Dorman, C. J. (2001) Requirement for the molecular adapter function of StpA at the *Escherichia coli* bgl promoter depends upon the level of truncated H-NS protein. Mol. Microbiol. **42**, 903–918
16 Nieto, J. M., Carmona, M., Bolland, S., Jubete, Y., de la Cruz, F. and Juárez, A. (1991) The *hha* gene modulates haemolysin expression in *Escherichia coli*. Mol. Microbiol. **5**, 1285–1293
17 Cornelis, G. R., Sluiters, C., Delor, I., Gelb, D., Kaninga, K., Lambert de Rouvroit, C., Sory, M. P., Vanooteghem, J. C. and Michiels, T. (1991) ymoA, a *Yersinia enterocolitica* chromosomal gene modulating the expression of virulence functions. Mol. Microbiol. **5**, 1023–1034
18 Nieto, J. M., Madrid, C., Prenafeta, A., Miquelay, E., Balsalobre, C., Carrascal, M. and Juárez, A. (2000) Expression of the hemolysin operon in *Escherichia coli* is modulated by a nucleoid–protein complex that includes the proteins Hha and H-NS. Mol. Gen. Genet. **263**, 349–358
19 Nieto, J. M., Madrid, C., Miquelay, E., Parra, J. L., Rodríguez, S. and Juárez, A. (2002) Evidence for direct protein–protein interaction between members of the enterobacterial Hha/YmoA and H-NS families of proteins. J. Bacteriol. **184**, 629–635
20 Paytubi, S., Madrid, C., Forns, N., Nieto, J. M., Balsalobre, C., Uhlin, B. E. and Juárez, A. (2004) YdgT, the Hha paralogue in *Escherichia coli* forms heteromeric complexes with H-NS and StpA. Mol. Microbiol. **54**, 251–263
21 Esposito, D., Petrovic, A., Harris, R., Ono, S., Eccleston, J. F., Mbabaali, A., Haq, I., Higgings, C. F., Hinton, J. C. D., Driscoll, P. C. and Ladbury, J. E. (2002) H-NS oligomerization domain structure reveals the mechanism for high order self-association of the intact protein. J. Mol. Biol. **324**, 841–850
22 Yee, A., Chang, X., Pineda-Lucena, A., Wu, B., Semesi, A., Le, B., Ramelot, T., Lee, G. M., Bhattacharyya, S., Gutierrez, P. et al. (2002) An NMR approach to structural proteomics. Proc. Natl. Acad. Sci. U.S.A. **99**, 1825–1830
23 Cantor, R. C. and Schimmel, P. R. (1980) Fluorescence anisotropy. In Biophysical Chemistry Part II: Techniques for the Study of Biological Structure and Function, pp. 463–466, W. H. Freeman and Co., San Francisco
24 Lakowicz, J. R. (1983) Protein fluorescence. In Principles of Fluorescence Spectroscopy (Rosenberg, A., ed.), pp. 357–359, Plenum Press, New York
25 Kuzmič, P. (1996) Program DYNAFIT for the analysis of enzyme kinetic data: Application to HIV proteinase. Anal. Biochem. **237**, 260–273
26 Loria, J. P., Rance, M. and Palmer, A. G. (1999) A relaxation-compensated Carr–Purcell–Meiboom–Gill sequence for characterizing chemical exchange by NMR spectroscopy. J. Am. Chem. Soc. **121**, 2331–2332
27 Goetlieb, H. E., Kotlyar, V. and Nudelman, A. (1997) NMR chemical shifts of common laboratory solvents as trace impurities. J. Org. Chem. **62**, 7512–7515
28 Bloch, V., Yang, Y., Margeat, E., Chavanieu, A., Augé, M. T., Robert, B., Arold, S., Rimsky, S. and Kochoyan, M. (2003) The H-NS dimerization domain defines a new fold contributing to DNA recognition. Nat. Struct. Biol. **10**, 212–218
29 Andersen, N. H., Neidigh, J. W., Harris, S. M., Lee, G. M., Liu, Z. and Tong, H. (1997) Extracting information from the temperature gradients of polypeptide NH chemical shifts: the importance of conformational averaging. J. Am. Chem. Soc. **119**, 8547–8561
30 Tsuda, S., Miura, A., Gagné, S. M., Spyracopoulos, L. and Sykes, B. D. (1999) Low-temperature-induced structural changes in the apo regulatory domain of skeletal muscle troponin C. Biochemistry **38**, 5693–5700
31 Malmendal, A., Evenas, J., Forsén, S. and Akke, M. (1999) Structural dynamics in the C-terminal domain of calmodulin at low calcium levels. J. Mol. Biol. **293**, 883–899
32 Yuan, T., Walsh, M. P., Sutherland, C., Fabian, H. and Vogel, H. J. (1999) Calcium-dependent and -independent interactions of the calmodulin-binding domain of cyclic nucleotide phosphodiesterase with calmodulin. Biochemistry **38**, 1446–1455

Received 4 January 2005/17 February 2005; accepted 18 February 2005
Published as BJ Immediate Publication 18 February 2005, DOI 10.1042/BJ20050002